THE JOURNAL OF BIOLOGICAL CHEMISTRY VOL. 287, NO. 24, pp. 20016–20026, June 8, 2012

Neutralizing Aspartate 83 Modifies Substrate Translocation of Excitatory Amino Acid Transporter 3 (EAAT3) Glutamate Transporters*[S]

Received for publication, January 19, 2012, and in revised form, April 13, 2012 Published, JBC Papers in Press, April 24, 2012, DOI 10.1074/jbc.M112.344077

Jasmin Hotzy[‡], Jan-Philipp Machtens[‡], and Christoph Fahlke[‡§1]

From the [‡]Institut für Neurophysiologie, Medizinische Hochschule Hannover, D-30625 Hannover, Germany and [§]Zentrum für Systemische Neurowissenschaften Hannover (ZSN), D-30559 Hannover, Germany

Background: Neutralizing a conserved aspartate between TM2 and TM3 affects gating of EAAT anion channels.
Results: Voltage clamp fluorometry demonstrates that the analogous mutation alters EAAT3 substrate translocation.
Conclusion: Altered substrate translocation is sufficient to explain anion channel gating in D83A EAAT3.
Significance: Dissection of transport and anion channel gating defines an intimate relationship between transporter translocation and anion channel opening.

Excitatory amino acid transporters (EAATs) terminate glutamatergic synaptic transmission by removing glutamate from the synaptic cleft into neuronal and glial cells. EAATs are not only secondary active glutamate transporters but also function as anion channels. Gating of EAAT anion channels is tightly coupled to transitions within the glutamate uptake cycle, resulting in Na^+- and glutamate-dependent anion currents. A point mutation neutralizing a conserved aspartic acid within the intracellular loop close to the end of transmembrane domain 2 was recently shown to modify the substrate dependence of EAAT anion currents. To distinguish whether this mutation affects transitions within the uptake cycle or directly modifies the opening/closing of the anion channel, we used voltage clamp fluorometry. Using three different sites for fluorophore attachment, V120C, M205C, and A430C, we observed time-, voltage-, and substrate-dependent alterations of EAAT3 fluorescence intensities. The voltage and substrate dependence of fluorescence intensities can be described by a 15-state model of the transport cycle in which several states are connected to branching anion channel states. D83A-mediated changes of fluorescence intensities, anion currents, and secondary active transport can be explained by exclusive modifications of substrate translocation rates. In contrast, sole modification of anion channel opening and closing is insufficient to account for all experimental data. We conclude that D83A has direct effects on the glutamate transport cycle and that these effects result in changed anion channel function.

Excitatory amino acid transporters (EAATs)[2] are secondary active transporters that mediate the stoichiometrically coupled transport of one glutamate, three sodium ions, and one proton while one potassium ion is countertransported (1, 2). They are necessary for termination of glutamatergic synaptic transmission and for maintenance of low resting glutamate levels (3–5). There are five different mammalian EAATs with distinct physiological roles. Genetic removal of mouse EAAT2 results in pronounced hyperexcitability and neurodegeneration (6), demonstrating the crucial role of this isoform for glutamate homeostasis in the central nervous system. Mouse models that lack other EAATs exhibit much milder phenotypes with certain impairment of motor coordination, behavioral abnormalities, or age-dependent neurodegeneration (7–10). EAAT3 is not only expressed in the central nervous tissue but also mediates glutamate and aspartate reabsorption in the renal proximal tubule (8). Naturally occurring mutations in the gene encoding EAAT3 cause human dicarboxylic aminoaciduria (11).

EAATs are not only glutamate transporters but also conduct a pore-mediated anion current (12–15). EAAT anion currents have been postulated to be involved in the regulation of cell excitability (16, 17), but so far, the physiological importance of this transport function is not sufficiently understood. Currently, EAAT anion currents are thought to be conducted through an anion pathway that is opened and closed in response to conformational changes underlying glutamate transport (18, 19). However, how this anion pore is formed and how opening and closing occur are unclear. In a systematic screen for mutations affecting EAAT1 anion channel function, D112A was found to abolish the glutamate dependence of EAAT1 anion currents (20). The corresponding mutation D117A was later shown to change unitary anion current amplitudes and relative anion selectivities of EAAT4 anion channels (19), suggesting close proximity of this residue to the EAAT4 anion conduction pathway. In addition to modifying EAAT1 anion currents, D112A reduces EAAT1 glutamate uptake rates by 40%.

So far, anion permeation through EAATs was thought not to affect glutamate transport (13). A mutation that changes anion conduction and coupled glutamate transport thus promises insights into the interdependence of the two EAAT transport

* This work was supported by Deutsche Forschungsgemeinschaft Grant FA301/9 (to Ch. F.).
[S] This article contains supplemental Figs. 1–3.
[1] To whom correspondence should be addressed: Inst. für Neurophysiologie, Medizinische Hochschule Hannover, Carl-Neuberg-Str. 1, D-30625 Hannover, Germany. Tel.: 49-511-532-2777; Fax: 49-511-532-2776; E-mail: fahlke.christoph@mh-hannover.de.
[2] The abbreviations used are: EAAT, excitatory amino acid transporter; TM, transmembrane domain; HP, hairpin.

functions, and thus, we decided to further study this mutation using voltage clamp fluorometry. Voltage clamp fluorometry combines electrophysiological and fluorescence measurements and has been used to monitor conformational changes in diverse transport proteins (21–23). We inserted the homologous mutation D83A into EAAT3 and applied voltage clamp fluorometry to separate the effects on coupled transport and on anion channel function. EAAT3 has already been studied using voltage clamp fluorometry, permitting detection of conformational rearrangements during coupled transport (23–26). Moreover, EAAT3 effectively transports glutamate (12, 27), thus permitting additional direct insights into the effects of neutralizing Asp-83 on coupled transport.

We found that D83A changes the time, substrate, and voltage dependence of EAAT3 fluorescence signals. Moreover, similar to earlier data on D112A EAAT1 and D117A EAAT4, D83A enlarged EAAT3 anion currents in the absence of glutamate but reduced glutamate-sensitive current amplitudes. It reduced coupled transport by about 50%. The data on fluorescence amplitudes and transport function can be described by a kinetic scheme in which only transitions within the uptake cycle are modified by the mutation, whereas the likelihood of anion channel opening was not changed in mutant transporters.

EXPERIMENTAL PROCEDURES

Expression of WT and Mutant hEAAT3 Transporters in Xenopus laevis Oocytes—Point mutations were introduced into pTLN2-hEAAT3 (28, 29) (kindly provided by Dr. Matthias Hediger (University of Bern, Switzerland)) using the QuikChange mutagenesis kit (Stratagene, La Jolla, CA). Capped cRNA was synthesized from MluI-/NheI-linearized pTLN2-hEAAT3 through use of mMESSAGE mMACHINE kits (Ambion, Austin, TX). Collagenase-treated, defolliculated stage IV-V oocytes were microinjected with 10 ng of RNA (Nanoliter 2000, World Precision Instruments, Sarasota, FL) and incubated at 18 °C in ND96 (96 mM NaCl, 2 mM KCl, 1.8 mM $CaCl_2$, 1 mM $MgCl_2$, 5 mM Hepes, pH 7.6 supplemented with 2.5 mM sodium pyruvate and 50 μg/ml gentamycin sulfate). Experiments were performed 3–7 days after injection.

Electrophysiology—Currents were recorded through two-electrode voltage clamp using a CA-1B amplifier (Dagan Corp., Minneapolis, MN) and digitized at 5 kHz using an ITC-18 computer interface in combination with Patchmaster (HEKA Elektronik, Lambrecht, Germany) (30). Experiments were performed under constant perfusion using a PF-8 eight-channel perfusion system (Abimek-Zech Electronic, Göttingen, Germany) with Ringer's solution (98.5 mM choline-Cl or NaCl/NO_3/gluconate, 1.8 mM $CaCl_2$/gluconate, and 1 mM $MgCl_2$/gluconate, 5 mM Hepes, pH 7.5, ±1 mM glutamate). Oocytes were held at 0 mV for at least 2 s between voltage steps.

Voltage Clamp Fluorometry—For fluorescence experiments, oocytes were labeled for 2–3 h with a 10 μM concentration of the fluorescent maleimide probe, Alexa Fluor 546 (Invitrogen). A short arc mercury lamp (HBO 103W/2, Osram, München, Germany) combined with a Uniblitz shutter (VS25S2ZMOR1-24 shutter, VCM-D1 shutter driver, Uniblitz, Vincent Assoc., Rochester, NY) was used as a light source. Fluorescence was monitored under voltage clamp by a photodiode (PIN020-A, AMS Technologies AG, Martinsried, Germany) and a rhodamine filter cube (HQ535/50x, Q565LP, HQ610/75m, Chroma Technology Corp., Bellows Falls, VT) attached to an inverted fluorescence microscope (IX71, Olympus, Hamburg, Germany). Fluorescence signals were amplified with a DLPCA-200 amplifier (Femto Messtechnik, Berlin, Germany) and low pass-filtered at 2 kHz (LPF-8, low pass Bessel filter, Warner Instruments, Hamden, CT). Representative fluorescence recordings were obtained by averaging 10 consecutive measurements.

Data Analysis—Electrophysiological and fluorescence data were analyzed with a combination of Patchmaster (HEKA Elektronik), pClamp10 (Molecular Devices, Sunnyvale, CA), MATLAB (The MathWorks, Natick, MA), and SigmaPlot (Jandel Scientific, San Rafael, CA). For statistical evaluations, Student's t test and paired t test with $p \leq 0.05$ (*) as the level of significance were used ($p \leq 0.01$ (**) and $p \leq 0.001$ (***)). The data are given as means ± S.E.

Kinetic Modeling—Voltage and substrate dependence of EAAT3 fluorescence was simulated by solving differential equations at steady state according to a previously developed 15-state model of EAAT2 extended by channel states branching from the uptake cycle (19, 23, 31). Rate constants of the uptake cycle were adopted from earlier work on cysteine-substituted EAAT3 (23). Anion channel open probabilities were estimated by optimizing the model against cysteine-substituted WT steady-state fluorescence data using the genetic algorithm as implemented in MATLAB (The MathWorks). The overall fluorescence was calculated as the sum of the products of relative fluorescence and probability of occupation for every state. This model was then adapted to D83A EAAT3 either by modifying translocation rates (reactions 8, 15, and 17) or anion channel open probabilities. In all cases, detailed balance was preserved, and fitting parameters were simultaneously optimized against experimentally determined relative glutamate uptake and anion current amplitudes. For kinetic modeling, we assumed the following intracellular concentrations: $[Na^+] = 10$ mM, $[K^+] = 70$ mM, [glutamate] = 12 mM, pH = 7.3 (1). Extracellular concentrations were set to experimental conditions.

RESULTS

Time, Substrate, and Voltage Dependence of EAAT-associated Currents and Fluorescence Signals—To permit site-directed fluorescence labeling of EAAT3, we introduced single cysteines into human EAAT3 and expressed WT and cysteine-substituted transporters in *Xenopus* oocytes (Fig. 1). We chose three reporter mutations localized in different parts of the transporter, V120C (3-4 loop), M205C (TM4c), and A430C (7-8 loop) (Fig. 1*A*), to observe fluorescence changes due to conformational changes in more than one protein region. M205C and A430C have already been used in earlier studies (23, 25), whereas V120C has not been reported to date. Because the fluorophore attachment site, Cys-120, is localized nearby an accessible endogenous cysteine, we additionally mutated Cys-158 to serine in all our constructs to prevent possible modifications by fluorophore application.

For each reporter mutation, the time course of fluorescence labeling was tested to define incubation times sufficient for

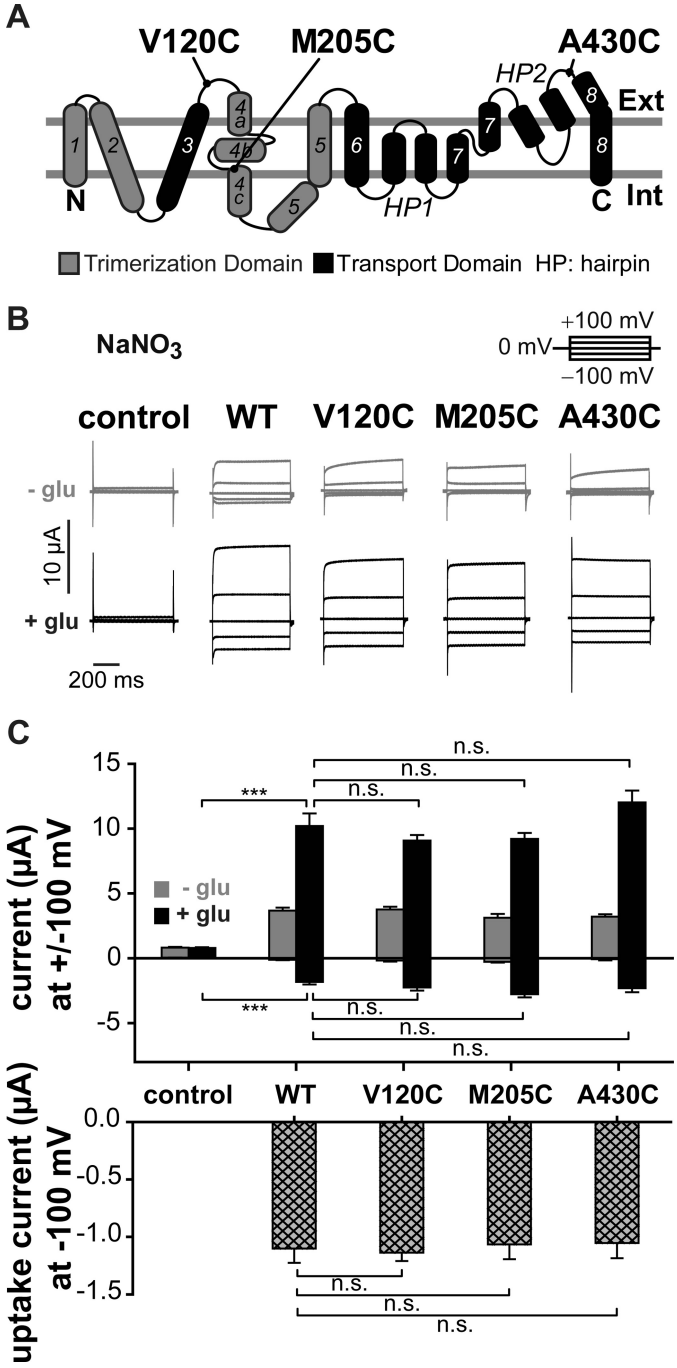

FIGURE 1. **Reporter mutations do not affect the function of EAAT3 associated currents.** *A*, localization of the fluorescence reporter mutations V120C, M205C, and A430C on the transmembrane topology model of EAAT3. The trimerization domain is shown in *gray*, and the transport domain and the hairpins are in *black*. *B*, representative current traces recorded from *X. laevis* oocytes expressing WT, V120C, M205C, or A430C EAAT3. *C*, averaged absolute current amplitudes at ±100 mV (*top*) and averaged uptake current amplitudes at −100 mV (*bottom*) calculated by the difference of measurements in sodium gluconate with and without glutamate. *n.s.*, not significantly different, $p > 0.05$; ***, $p \leq 0.001$. Data are given as means ± S.E.; $n \geq 7$. *Int*, internal; *Ext*, external; *glu*, glutamate.

maximum labeling (supplemental Fig. 1). V120C, M205C, and A430C EAAT3-injected oocytes exhibited higher levels of fluorescence intensities than uninjected oocytes or oocytes expressing C158S EAAT3 (data not shown). Moreover, oocytes expressing V120C, M205C, or A430C EAAT3 displayed fluorescence changes upon voltage or substrate alterations (supplemental Fig. 2) that were absent in uninjected oocytes or those expressing C158S EAAT3, indicating that cysteine-substituted EAAT3 is specifically labeled with the fluorescent dye.

To test whether cysteine insertions change glutamate transport or anion conduction, we studied WT and cysteine-substituted EAAT3 currents using two-electrode voltage clamp (Fig. 1*B*). Application of glutamate resulted in a pronounced increase of current amplitudes at negative as well as at positive voltages. In the absence as well as in the presence of glutamate, current amplitudes in oocytes expressing V120C, M205C, or A430C EAAT3 were not statistically different from those of WT EAAT3, illustrating comparable expression levels. EAAT3 currents consist of two components, glutamate uptake currents due to electrogenic transport and EAAT3-associated anion currents. Glutamate uptake current can be separated from anion currents after substituting permeant anions with impermeant gluconate and measured as the difference of currents in the presence and in the absence of glutamate (2, 13, 33). Glutamate uptake is strongly voltage-dependent and decreases to values around zero at positive potentials (2). Thus, currents at positive voltages predominantly represent anion currents. The use of NO_3^- as the main external anion results in EAAT3 currents that are significantly larger than endogenous currents of uninjected oocytes and permit accurate measurements of EAAT3 anion currents (Fig. 1*B*) (33). For all tested constructs, glutamate uptake currents and anion currents at saturating glutamate concentrations were not statistically different from WT values, illustrating that none of the cysteine substitutions modify functional properties of EAAT3 (23, 25) (Fig. 1, *B* and *C*).

Fig. 2 shows representative fluorescence recordings from V120C, M205C, or A430C EAAT3 in the absence (*top*) or in the presence (*bottom*) of 1 mM L-glutamate. Oocytes were held at 0 mV, and voltage steps between −150 mV and +150 mV were applied in 50-mV intervals. In the absence of glutamate, hyperpolarizing voltage steps caused a slow reduction of V120C EAAT3 fluorescence that could be fit with a monoexponential function ($\tau_{(-150\ mV)} = 46.7 \pm 4.3$ ms, $n = 3$) (Fig. 2*A*). M205C and A430C EAAT3 exhibited fluorescence amplitudes that, in the absence of glutamate, increased upon membrane depolarization and decreased upon hyperpolarization (Fig. 2, *B* and *C*). The time course of these voltage-dependent changes was significantly faster than for V120C ($\tau_{(M205C,\ -150/+150\ mV)} = 4.3 \pm 0.4/7.1 \pm 0.9$ ms, $n = 3$; $\tau_{(A430C,\ -150/+150\ mV)} = 10.5 \pm 0.6/8 \pm 1.2$ ms, $n = 3$). For M205C EAAT3, the initial rise upon membrane depolarization was followed by a much slower decay (Fig. 2).

Application of glutamate increased fluorescence intensities of V120C EAAT3 and decreased these values for M205C and A430C EAAT3. Glutamate modified the voltage dependences of fluorescence signals for all cysteine-substituted EAAT3 constructs (Fig. 2). Application of L-glutamate accelerated the time course of fluorescence change ($\tau_{(+150\ mV)} = 16 \pm 0.5$ ms, $n = 3$) and modified its voltage dependence for V120C EAAT3 (Fig. 2*A*). For M205C and A430C EAAT3 (Fig. 2, *B* and *C*), fluorescence showed the lowest intensity around 0 mV and increased upon positive as well as negative membrane potentials. In the presence of glutamate, fluorescence increased on a slow time

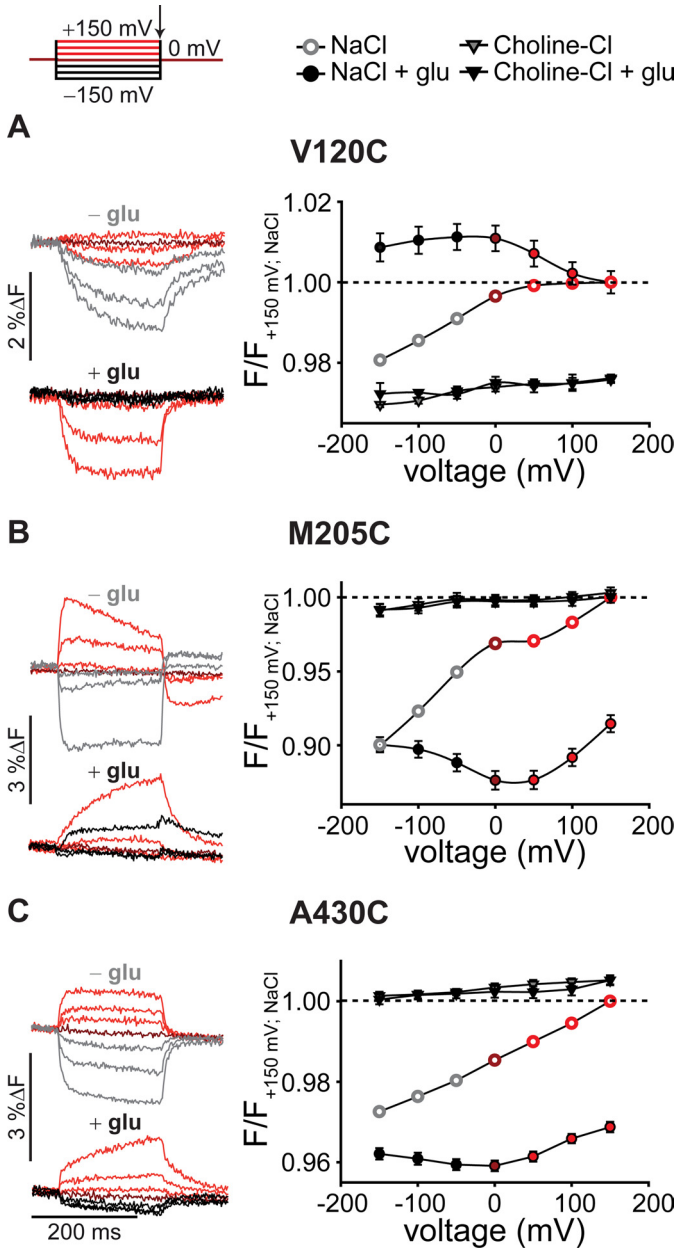

FIGURE 2. **Voltage- and substrate-dependent conformational changes of EAAT3.** Representative fluorescence traces (*left column*) recorded from *X. laevis* oocytes expressing V120C (*A*), M205C (*B*), and A430C EAAT3 (*C*) and averaged voltage dependence of late (*arrow*) relative fluorescence changes (*right column*) in the presence of different substrates are shown. Fluorescence signals were measured in NaCl Ringer's solution during 200-ms voltage steps between +150 and −150 mV. Fluorescence amplitudes were normalized to the fluorescence generated at +150 mV in NaCl solution. Measurements in NaCl at voltages above 0 mV are shown in *red*, 0 mV is in *dark red*, and negative voltages in the absence of 1 mM glutamate are shown in *light gray* and in the presence of 1 mM glutamate are shown in *black*. Fluorescence data from at least six oocytes are reported as means ± S.E. *F*, fluorescence; *glu*, glutamate.

course upon depolarization as well as upon hyperpolarization ($\tau_{(M205C,\ +150\ mV)}$ = 87.2 ± 3.2 ms, n = 3; $\tau_{(A430C,\ +150\ mV)}$ = 59.2 ± 4.2 ms, n = 2).

EAAT-mediated glutamate transport is based on a series of substrate association steps and related conformational changes. Three Na^+ ions, one H^+, and one glutamate associate with the outward facing transporter with an open extracellular gate (hairpin 2 (HP2)). After closure of HP2 and movement of the translocation domain to the inside (34), Na^+, H^+, and glutamate are released by opening of the intracellular gate (hairpin 1 (HP1)), and the uptake cycle is completed by retranslocation after association of K^+ or Na^+. Modification of the uptake cycle by removal of certain substrates or application of EAAT-specific blockers allows testing of the specificity of the observed signals. For all constructs, substitution of Na^+ by choline$^+$ abolished the voltage dependence of fluorescence signals and changed the fluorescence intensity (Fig. 2). A specific blocker of EAAT transporters, DL-*threo*-benzyloxyaspartate (35, 36), inhibited fluorescence changes in the absence and in the presence of glutamate by about 90%, supporting the notion that fluorescence changes are due to conformational rearrangements in the glutamate transporter (supplemental Fig. 2).

EAAT4 anion channel gating depends on anion concentrations on both membrane sites (19, 33). To test whether EAAT3 fluorescence intensities undergo anion-dependent alterations, we studied all cysteine-substituted EAAT3 constructs after substitution of the external anion by gluconate. Chloride removal did not change the intensity or voltage dependence of fluorescence signals (supplemental Fig. 3, A–C). We conclude that fluorescence changes of fluorophores added to V120C, M205C, and A430C report on conformational changes within the EAAT3 uptake cycle that require external Na^+ but do not depend on the anion composition.

Voltage Clamp Fluorometry Reveals Additional Slow Conformational Changes—In addition to the initial rise upon depolarization, fluorescence intensities of M205C EAAT3 exhibited voltage-dependent changes with a very slow time course. Fig. 3 shows such current and fluorescence recordings of M205C EAAT3 on an extended time scale. In the absence of glutamate, a depolarizing voltage step to +50 mV caused a very slow fluorescence decay ($\tau_{(+50\ mV)}$ = 6.7 ± 1.2 s, n = 6). This process is not due to bleaching because we observed slow fluorescence recovery upon return to the holding potential of 0 mV (Fig. 3*A*). Application of glutamate shifted the voltage dependence of these slow processes so that relaxation of these signals was observed upon voltage steps to −100 mV ($\tau_{(-100\ mV)}$ = 4.0 ± 1.2 s, n = 11) (Fig. 3*A*).

These fluorescence changes are too slow to represent transitions within the uptake cycle. However, we did not observe slow fluorescence changes in the absence of transport substrates or in the presence of DL-*threo*-benzyloxyaspartate (supplemental Fig. 2), suggesting that the slow fluorescence signal also reflects conformational changes coupled to the uptake cycle. A possible explanation might be a conformational change occurring from certain states of the uptake cycle. Such a kinetic scheme predicts that occupation of this novel state will prevent progress of the uptake cycle and thus result in concomitant slow alterations of transport rates. We tested for slow voltage-dependent changes of glutamate transport rates by studying glutamate uptake currents after prepulses to positive voltages. These experiments were performed in external gluconate after incubation of oocytes in Cl^--free solution (13). For various pulse protocols, we did not observe any time- or voltage-dependent changes in transport current amplitudes (Fig. 3*B*). These data indicate that slow fluorescence changes cannot be represented as transitions branching from the uptake cycle.

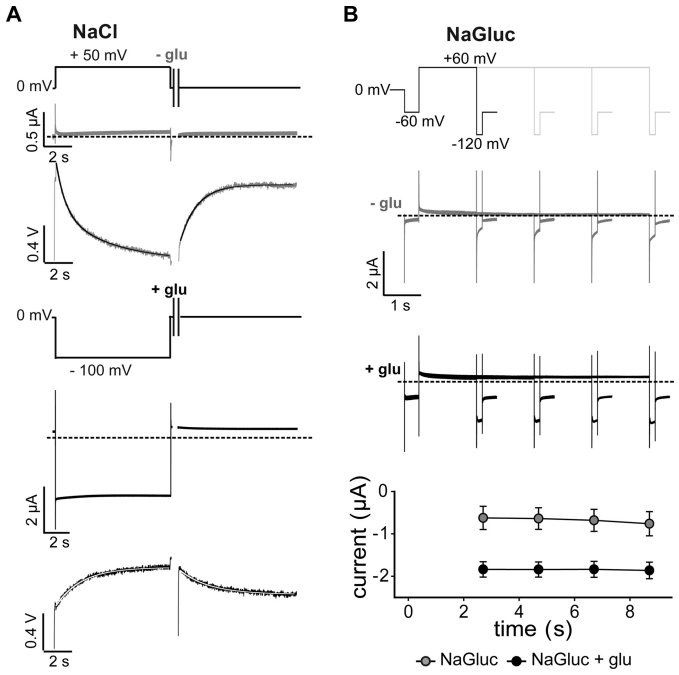

FIGURE 3. **Slow conformational changes in EAAT3.** *A*, representative current and fluorescence traces recorded from *X. laevis* oocytes expressing M205C EAAT3 in response to long voltage steps to +50 mV in the absence of glutamate (*light gray*; *top*) or to −100 mV in the presence of glutamate (*black*; *bottom*) and the recovery back to the holding potential of 0 mV. *B*, current responses to voltage steps to +60 mV of increasing durations followed by fixed test steps to −120 mV in the absence of glutamate (*light gray*; *top*) and in the presence of glutamate (*black*; *middle*). Averaged current amplitudes (*bottom*) are given as means ± S.E.; $n = 4$. *glu*, glutamate; *NaGluc*, sodium gluconate.

D83A Modifies EAAT3 Glutamate Transport, Anion Currents, and Fluorescence Amplitudes—We next inserted the D83A mutation into each cysteine-substituted EAAT3 construct and studied the functional effects of this mutation using voltage clamp analysis. Asp-83 is localized between TM2 and TM3 and is highly conserved among mammalian EAATs (Fig. 4*A*). Because homologous mutations in EAAT1 (20) and EAAT4 (19) alter glutamate transport and anion conduction, D83A might allow insights into how conformational changes underlying coupled transport open and close the anion channel.

At positive membrane potentials in the absence of glutamate, D83A EAAT3 currents were statistically larger than WT or cysteine-substituted EAAT3 currents (Fig. 4, *B* and *C*) (WT (3.7 ± 0.2 µA) compared with V120C,D83A (7.7 ± 0.3 µA), $p < 0.001$; compared with M205C,D83A (6.1 ± 0.5 µA), $p = 0.006$; and compared with A430C,D83A (9.5 ± 0.5 µA), $p < 0.001$; $n > 10$). The glutamate-induced current increase was less pronounced in D83A EAAT3 than in WT EAAT3 (Fig. 4*C*, *top*). This is due to virtually glutamate-independent anion current amplitudes (Fig. 4*C*, *middle*). Moreover, D83A reduced uptake current amplitudes to values between 30 and 50% for all reporter mutations (Fig. 4*C*, *bottom*).

Voltage clamp fluorometry revealed D83A-induced changes in the voltage and substrate sensitivity of the fluorescence signals for each fluorophore attachment site (Fig. 5). V120C,D83A and A430C,D83A EAAT3 fluorescence signals increased during depolarization and decrease during hyperpolarization (Fig. 5, *A* and *C*). However, D83A modified the time course of hyperpolarization-induced fluorescence decreases (($\tau_{(V120C,D83A,\ -150\ mV)}$ = 18.2 ± 2.6 ms, $n = 2$; $\tau_{(A430C,D83A,\ -150/+150\ mV)}$ = 12.7 ± 2.6/11.5 ± 2.8 ms, $n = 4$). The voltage dependence of M205C EAAT3 fluorescence was dramatically altered by D83A. Without external glutamate, D83A EAAT3 fluorescence amplitudes displayed minimum levels around +50 mV and increased with depolarization and hyperpolarization to nearly the same intensity as in sodium-free conditions (Fig. 5*B*). Furthermore, the maximum change of fluorescence intensity by applying different membrane potentials was less pronounced than for M205C EAAT3 (5% instead of 10%).

Glutamate decreased the fluorescence intensity of V120C,D83A and M205C,D83A EAAT3 and modified their voltage dependences (Fig. 5, *A* and *B*). Whereas fluorescence signals of V120C,D83A and M205C,D83A EAAT3 require external Na^+, A430C,D83A EAAT3 voltage-dependent fluorescence changes seemed to be less substrate-dependent (Fig. 5*C*). Removal of external permeant anions did not affect the intensity or the voltage dependence of fluorescence signals of D83A EAAT3 (supplemental Fig. 3, D–F), similar to our results on EAAT3 with an aspartate at position 83.

Kinetic Modeling Reveals Changes in Glutamate Uptake Cycle in D83A EAAT3—Glutamate transport by EAATs can be described with a kinetic scheme that encompasses subsequent substrate association/dissociation and translocation steps between inward and outward facing conformations (14, 31, 37) (Fig. 6). Anion channel gating is tightly coupled to these transitions and can be represented by adding branching open anion channel states (19, 38, 39). Because the transport cycle can only proceed from closed channel states (19, 38), opening of EAAT anion channels prevents progression of the uptake cycle. Changes in the distribution between open and closed anion channel states will therefore affect the uptake cycle.

D83A could alter EAAT3 function by directly modifying substrate association/dissociation or transporter translocation rates. Alternatively, D83A might modify apparent transitions within the uptake cycle by changing anion channel opening and closing transitions. To distinguish between the two possibilities, sole modification of transitions within the uptake cycle or modification by changed anion channel open probabilities, we modeled voltage-dependent fluorescence data from WT and D83A EAAT3 with a kinetic model that is based on a scheme developed to describe EAAT3 fluorescence data (23).

We modified this model by increasing the number of different fluorescence levels for each fluorescently labeled transporter from three to four. The four fluorescence levels of our kinetic scheme correspond to four structurally distinct conformations (Fig. 6). The empty transporter resides in an outward facing state with HP2 open and the substrate binding sites exposed to the extracellular space (Fo_{open}: ToK and To). Glutamate uptake is initiated by association of three Na^+ ions, one H^+, and one glutamate. Association of these substrates causes closure of HP2 ($Fo_{occluded}$: ToNa1, ToNa2, ToNa2G, ToNa2H, ToNa2GH, and ToNa3GH), and a large piston-like movement of the "translocation domain" results in the inward facing conformation ($Fi_{occluded}$: TiNa3GH, TiNa2GH, TiNa2G, TiNa2,

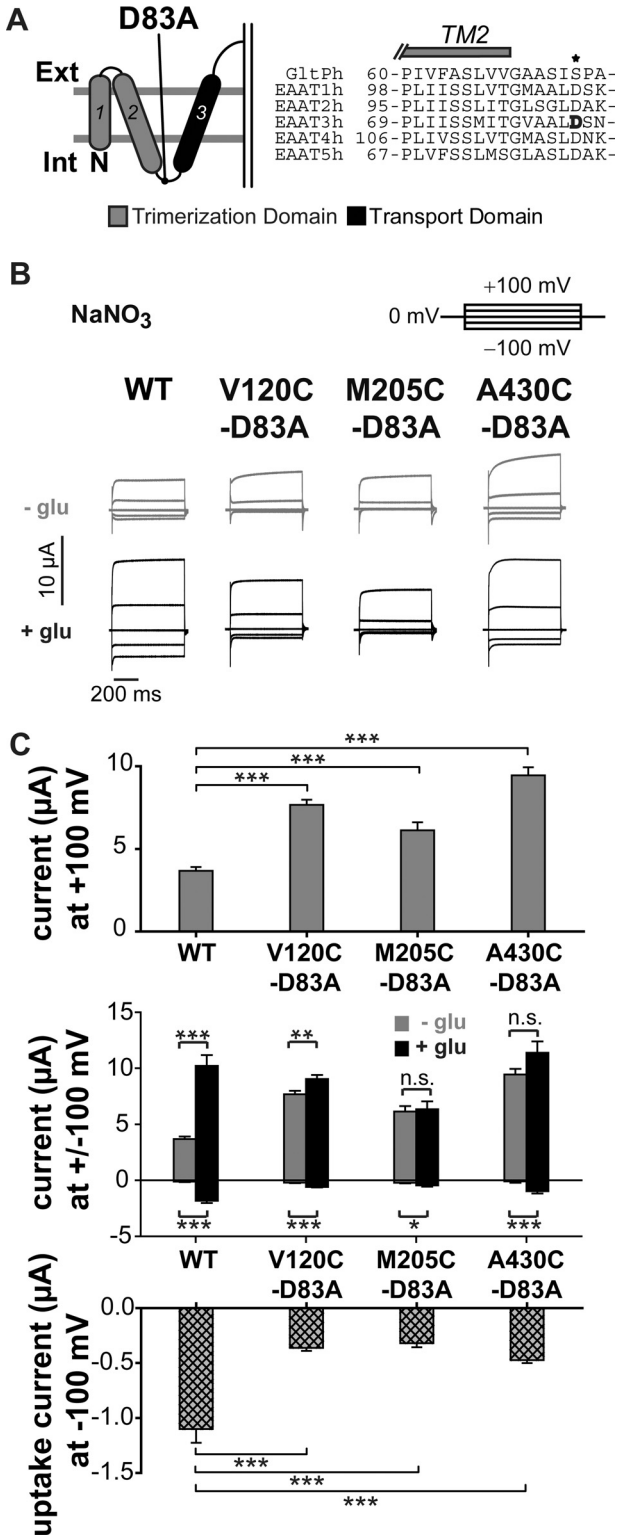

FIGURE 4. **D83A changes substrate dependence of EAAT3 current amplitudes.** *A*, localization of the mutation D83A in the transmembrane topology model. The trimerization domain is shown in *gray*, and the transport domain is shown in *black*. The amino acid sequence alignment of Glt_{Ph} and EAAT1–5 shows the TM2-TM3 region. Asp-83 of EAAT3 is highlighted in *black*. *B*, representative current traces recorded from *X. laevis* oocytes expressing V120C,D83A, M205C,D83A, or A430C,D83A EAAT3. *C*, averaged absolute current amplitudes at ±100 mV with and without glutamate (*top*), averaged relative glutamate-induced current increase at +100 mV (*middle*) calculated by division of the current in the presence of glutamate by the current in the absence of glutamate, and averaged uptake current amplitudes at −100 mV (*bottom*) calculated by the difference of currents in sodium gluconate with and without glutamate from oocytes expressing WT or mutant EAAT3. *n.s.*, not significantly different, $p > 0.05$; *, $p \leq 0.05$; **, $p \leq 0.01$; ***, $p \leq 0.001$. Data are given as means ± S.E.; $n \geq 10$. *Int*, internal; *Ext*, external; *glu*, glutamate.

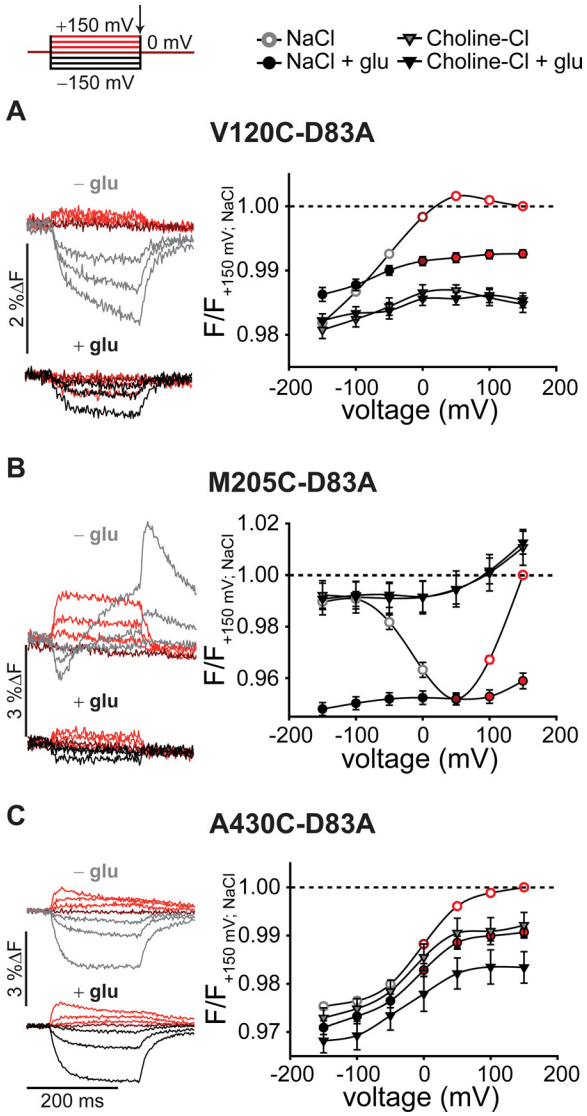

FIGURE 5. **Voltage- and substrate-dependent conformational changes of D83A EAAT3.** Representative fluorescence traces (*left column*) recorded from *X. laevis* oocytes expressing V120C,D83A (*A*), M205C,D83A (*B*), and A430C,D83A EAAT3 (*C*) and averaged voltage dependence of late (*arrow*) relative fluorescence changes (*right column*) in the presence of different substrates are shown. Fluorescence signals were measured in NaCl Ringer's solution during 200-ms voltage steps between +150 and −150 mV. Fluorescence amplitudes were normalized to the fluorescence generated at +150 mV in NaCl solution. Measurements in NaCl at voltages above 0 mV are shown in *red*, 0 mV is shown in *dark red*, and negative voltages in the absence of 1 mM glutamate are shown in *light gray* and in the presence of 1 mM glutamate are shown in *black*. Fluorescence data from at least six oocytes are reported as means ± S.E. *F*, fluorescence; *glu*, glutamate.

and TiNa1) (26). Opening of HP1 is followed by substrate release and exposure of the binding sites to the intracellular solution (Fi_{open}: Ti and TiK) (23). Retranslocation after association of internal K^+ completes the uptake cycle. The gating of EAAT anion channels can be represented by adding branching open channel states from the uptake cycle (Fig. 6, *A* and *B*) (19,

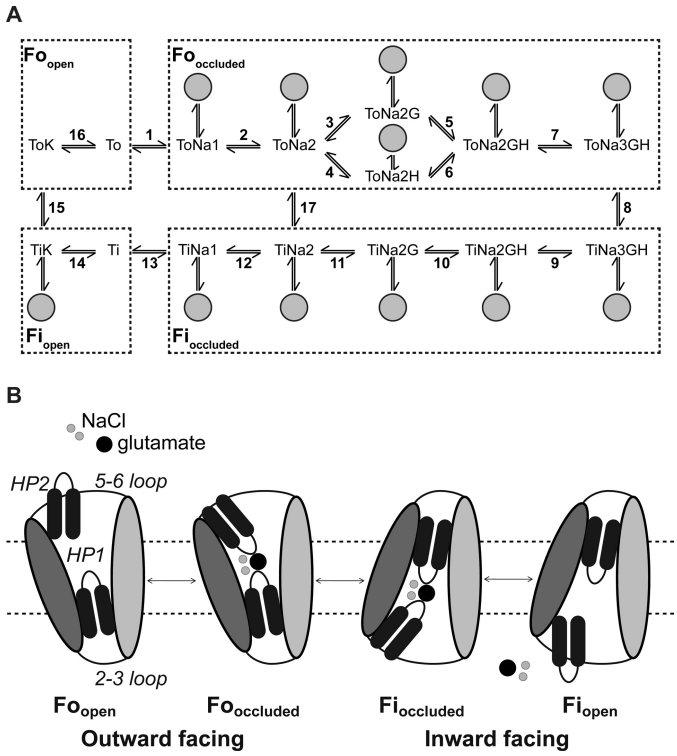

FIGURE 6. **Kinetic model and transport scheme of wild type and mutant EAAT3.** *A*, modified 15-state model extended by anion channel states branching from states 2–12 and state 14 (*gray circles*) (16, 28) used to simulate the fluorescence data. *B*, schematic transport mechanism. Shown is a single protomer. The isomerization between the outward and inward facing occluded states occurs upon movement of the whole transport domain (*dark gray*) relative to the trimerization domain (*light gray*). The inward facing open state has not been structurally characterized and is hypothetical (modified from Reyes *et al.* (34).

38). Anion channel opening and closing are assumed to be fast compared with transitions in the uptake cycle, and therefore, we only used probabilities of anion channel opening from a particular state. These state-specific open probabilities are ratios of the number of transporters in one transporter state with an open anion channel to the total number of transporters in this particular state with either an open or a closed channel.

To obtain a kinetic scheme describing fluorescence values, anion currents, and uptake currents for WT EAAT3, we used the same rate constants of the uptake cycle as determined in earlier work on cysteine-substituted EAAT3 (23). We determined anion channel open probabilities by fitting the model to the experimentally observed fluorescence of V120C, M205C, and A430C EAAT3. The parameters were constrained to correctly describe experimentally determined relative glutamate-induced current amplitudes at +100 mV and to preserve detailed balance (Fig. 7*G*). The so-obtained fitting parameters (Tables 1, 2, and 3) demonstrated a good agreement of the simulated and observed fluorescence-voltage relationship under different substrate conditions (Fig. 7, *A–C*). However, they predicted a transport rate of about four transported glutamates per second at −100 mV (Fig. 7*H*), which is lower than in previously published data relating to EAAT1, -2, or -3 (27, 40). We did not succeed in modifying fit parameters to increase transport rates. All attempts impaired the compatibility with the experimentally observed voltage dependence of fluorescence. Because unitary transport currents are extremely difficult to measure directly, we accepted this deviation between published and predicted results and only used the relative decrease of glutamate uptake currents by D83A in the optimization procedure.

We then modified the thus established kinetic model to account for the fluorescence signals and transport properties of D83A EAAT3. We initially tested whether modifying reactions in certain parts of the uptake cycle can qualitatively account for the observed D83A-mediated changes in fluorescence. There were two processes that resulted in such alterations, changes in anion channel open probability and changes in translocation rates.

We first optimized all anion channel opening/closing reactions simultaneously against fluorescence intensities for all three reporter mutations combined with D83A. Glutamate-induced increases of anion current amplitudes at +100 mV, relative glutamate uptake currents at −100 mV, and detailed balance were again used as constraints. During optimization of opening and closing rates of anion channels, global fitting yielded a set of parameters that well reproduced the fluorescence-voltage relationship of D83A EAAT3 under different ionic conditions. However, these changes always predicted reduction of glutamate transport rates to negligible values. Therefore, we evaluated whether alterations of translocation rates within the uptake cycle can account for D83A fluorescence and function. In these fitting procedures, only the three translocation reactions were adjusted. The fitting procedure revealed altered translocation rates of the K^+-bound (reaction 15), the Na^+-bound (reaction 17), and the Na^+- and glutamate-bound transporter (reaction 8). Whereas inward translocation from ToNa3GH to TiNa3GH was promoted, D83A stimulated the outward translocation for the two other processes (Tables 1–3). These alterations resulted in predicted fluorescence data that resemble experimental data on D83A EAAT3 (Fig. 7, *D–F*, and Tables 1–3).

The kinetic model permits the prediction of the steady-state probability that the transporter resides in a given state of the transport cycle. We next calculated the residence probability of each state of the uptake cycle under steady-state conditions for the cysteine-substituted WT (Fig. 7*I*) or D83A EAAT3 (Fig. 7*J*). In the presence as well as in the absence of glutamate, D83A EAAT3 was predicted to reside with higher likelihood in the inward facing conformation than cysteine-substituted EAAT3.

DISCUSSION

Here, we studied the functional consequences of neutralizing a conserved aspartate at position 83 in EAAT3. Homologous mutations have already been studied in EAAT1 and EAAT4 (19, 20) and were reported to result in dramatic alterations of EAAT anion channel opening and closing for both isoforms. Investigating the effects of this point mutation on conformational changes promised insights into the interaction of transporter and anion channel function of EAAT glutamate transporters.

In our experiments, transporter proteins were labeled with fluorophores, and fluorescence intensities were measured upon changes in membrane voltages or in substrate concentrations

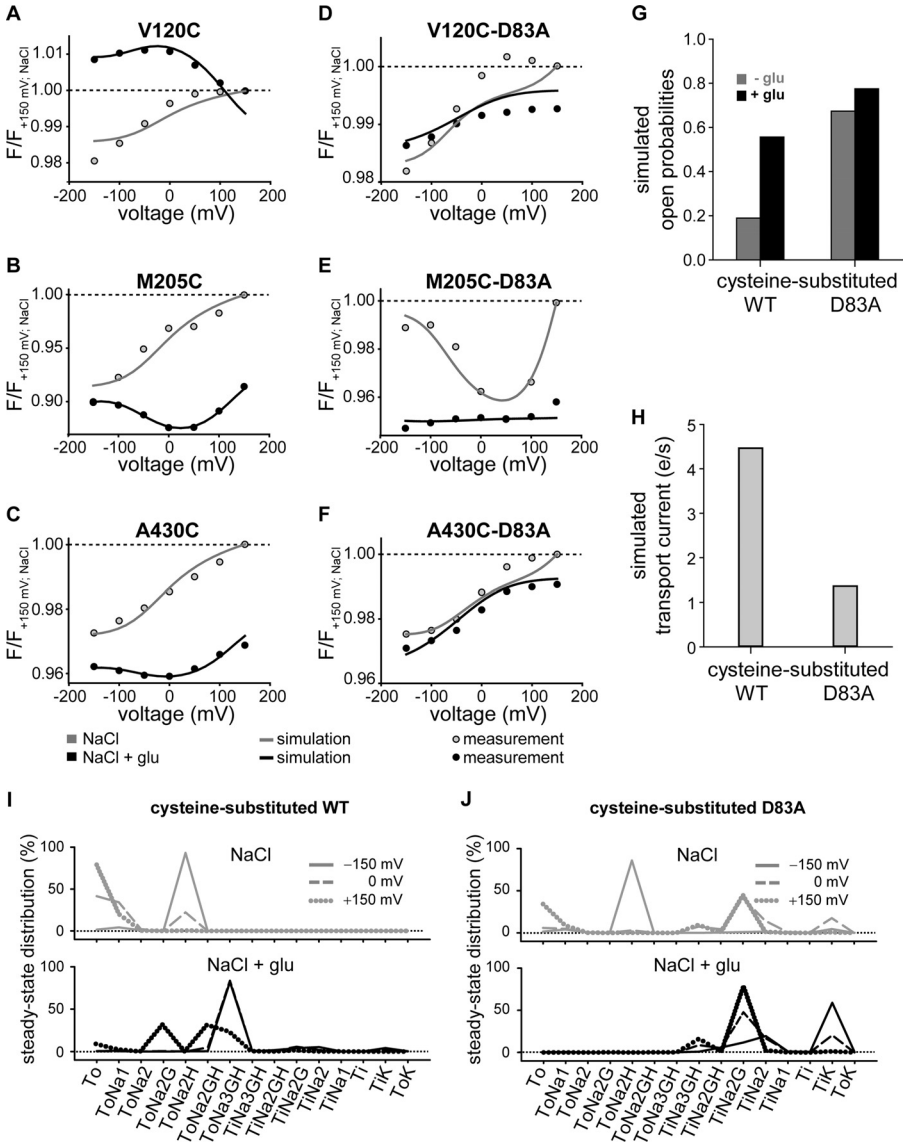

FIGURE 7. **Simulated voltage- and substrate-dependent conformational changes, open probabilities and transport currents of cysteine-substituted and D83A EAAT3.** *A–F*, averaged voltage dependence of measured late fluorescence changes (fluorescence-voltage relationship) (*circles*) and simulated fluorescence changes (*solid lines*) in the absence (*gray*) or in the presence of 1 mM glutamate (*black*). Fluorescence amplitudes were normalized to the fluorescence generated at +150 mV in NaCl solution. *G* and *H*, simulated open probabilities (*G*) at +100 mV of cysteine-substituted WT and D83A EAAT3 without (*gray*) and in the presence of glutamate (*black*) and simulated transport currents (*H*) at −100 mV from the data given in Tables 1 and 3. *e*, elementary change; $e = 1.602\,176\,462(63)\cdot10^{-19}$C. *I* and *J*, simulated residence probability of cysteine-substituted WT (*I*) and D83A EAAT3 (*J*) calculated from the data given in Table 1 without (*gray*) and in the presence of glutamate (*black*) for three different voltages, −150 (*solid line*), 0 (*dashed line*), and +150 mV (*dotted line*). *glu*, glutamate; *F*, fluorescence.

(22, 41). We used three different cysteine substitutions, V120C, M205C, and A430C, for these experiments. Labeling of cysteine-substituted EAAT3 was specific because the same procedures on oocytes expressing EAAT3 that lack cysteines for fluorophore attachment resulted in background fluorescence levels (supplemental Figs. 1 and 2). For each reporter mutant, voltage steps caused changes in fluorescence amplitudes that were modified by concentrations of transporter substrates, such as Na^+ and glutamate (Fig. 2). Moreover, application of DL-*threo*-benzyloxyaspartate abolished our observed fluorescence changes (supplemental Fig. 2). Because DL-*threo*-benzyloxyaspartate is known to lock EAATs into an outward facing conformation with HP2 open (35) and thus to prevent substrate binding and subsequent voltage-dependent conformational changes, this result further supports the notion that fluorescence signals arise from conformational changes of the EAAT3 transporter.

Because EAATs are dual function proteins, the observed fluorescence changes might report on transitions within the uptake cycle or on anion channel opening and closing. We found that the voltage and substrate dependence of EAAT3 fluorescence signals can be well described by a kinetic model that is based on the glutamate transport cycle and in which opening and closing transitions of anion channels are voltage-independent (Fig. 6) (5, 23, 34). Moreover, fluorescence is modified by transport substrates that affect the transport cycle but do not directly affect the anion channel opening and closing (42). Taken together, these results indicate that the observed

TABLE 1

Parameters of EAAT3 model

Rate constants of the transport process and channel opening/closing at −70 mV are shown. Electrogenic reactions are defined by $z\delta$ values, which correspond to the product of the charge and the fraction of the electric field the charge is moved across the membrane. Clockwise transitions in the model scheme are denoted as "forward reactions."

				Changed parameters for D83A	
Reaction	Forward	Backward	$z\delta$	Forward	Backward
1	$1.00 \cdot 10^4$ M^{-1} s^{-1}	$2.50 \cdot 10^3$ s^{-1}	0.20		
2	$1.00 \cdot 10^4$ M^{-1} s^{-1}	$2.50 \cdot 10^3$ s^{-1}	0.20		
3	$6.80 \cdot 10^6$ M^{-1} s^{-1}	$3.00 \cdot 10^2$ s^{-1}	−0.40		
4	$6.00 \cdot 10^{11}$ M^{-1} s^{-1}	$7.00 \cdot 10^2$ s^{-1}			
5	$6.00 \cdot 10^{11}$ M^{-1} s^{-1}	$7.00 \cdot 10^2$ s^{-1}	0.40		
6	$6.80 \cdot 10^6$ M^{-1} s^{-1}	$3.00 \cdot 10^2$ s^{-1}			
7	$1.00 \cdot 10^4$ M^{-1} s^{-1}	$1.00 \cdot 10^3$ s^{-1}	0.55		
8	$5.50 \cdot 10^2$ s^{-1}	$5.00 \cdot 10^2$ s^{-1}		$1.00 \cdot 10^5$ s^{-1}	6.59 s^{-1}
9	$8.00 \cdot 10^2$ s^{-1}	$4.00 \cdot 10^4$ M^{-1} s^{-1}	0.45		
10	$6.00 \cdot 10^3$ s^{-1}	$9.00 \cdot 10^{10}$ M^{-1} s^{-1}			
11	$3.00 \cdot 10^3$ s^{-1}	$4.00 \cdot 10^5$ M^{-1} s^{-1}			
12	$5.00 \cdot 10^2$ s^{-1}	$2.00 \cdot 10^5$ M^{-1} s^{-1}			
13	$4.00 \cdot 10^3$ s^{-1}	$1.00 \cdot 10^6$ M^{-1} s^{-1}	0.20		
14	$1.00 \cdot 10^6$ M^{-1} s^{-1}	$1.00 \cdot 10^3$ s^{-1}			
15	50 s^{-1}	5.00 s^{-1}	0.40	131.45 s^{-1}	$1.00 \cdot 10^5$ s^{-1}
16	$8.00 \cdot 10^2$ s^{-1}	$1.00 \cdot 10^4$ M^{-1} s^{-1}			
17	0.80 s^{-1}	$1.00 \cdot 10^{-2}$ s^{-1}		0.11 s^{-1}	19.19 s^{-1}

TABLE 2

Fluorescence intensities used for simulations of cysteine-substituted wild type and mutant EAAT3 fluorescence-voltage relationships

Fluorescence intensities of fluorescence states $Fo_{open/occluded}$ and $Fi_{open/occluded}$ of cysteine-substituted and D83A EAAT3 used to simulate the overall fluorescence-voltage relationship were normalized to the fluorescence intensity of Fo_{open}.

Fluorescence state	V120C	M205C	A430C	V120C,D83A	M205C,D83A	A430C,D83A
Fo_{open}	1.00	1.00	1.00	1.00	1.00	1.00
$Fo_{occluded}$	0.98	0.89	0.96	0.97	0.92	0.96
$Fi_{occluded}$	1.32	0.29	0.79	0.98	0.88	0.97
Fi_{open}	0.52	2.44	1.25	0.97	0.88	0.93

TABLE 3

State-specific probabilities for channel opening used in kinetic modeling of cysteine-substituted wild type and mutant EAAT3

Anion channel state branching from	Open probability
ToNa1	0.722
ToNa2	$9.999 \cdot 10^{-5}$
ToNa2G	$9.999 \cdot 10^{-5}$
ToNa2H	$9.999 \cdot 10^{-5}$
ToNa2GH	$1.321 \cdot 10^{-4}$
ToNa3GH	0.988
TiNa3GH	0.826
TiNa2GH	0.713
TiNa2G	$1.275 \cdot 10^{-4}$
TiNa2	$1.008 \cdot 10^{-4}$
TiNa1	0.765
TiK	$1.357 \cdot 10^{-4}$

fluorescence changes are not directly linked to opening and closing of the anion channel.

Time courses of fluorescence changes are therefore expected to reflect rate constants of transitions between individual states of the uptake cycle. However, we observed different kinetics but very similar voltage dependences of fluorescence changes of M205C and A430C (Fig. 2, *B* and *C*). The time dependences of fluorescence amplitudes obviously depend not only on global conformational changes of the EAAT proteins but also on additional region-specific changes of the environment. We therefore did not use the time dependence of fluorescence amplitudes to deduce information about rate constants within the uptake cycle.

For M205C EAAT3, we observed very slow changes in the fluorescence amplitude upon depolarizing voltage steps in the absence of external glutamate and upon membrane hyperpolarization after application of glutamate (Fig. 3). The time dependence of this process can be well described with a single time constant of around 7 s without glutamate and around 4 s in the presence of the substrate. Turnover rates of individual EAAT3 proteins have been determined to be well above 10/s (27), and such slow time constants thus indicate a conformational change outside the transport cycle. Because ultraslow fluorescence changes are voltage-dependent (Fig. 3*A*) and because glutamate modifies this voltage dependence, one might speculate about the existence of a branching connection from one of the states of the uptake cycle. After entering such a branching state, the transport cycle is interrupted and can only resume after having left this particular long lasting state. We tested the existence of such a branching connection by measuring time-dependent changes in glutamate transport currents. The existence of long lasting branching states requires that glutamate transport rates are changed with the same time constant as the fluorescence signal. However, we did not observe any time- or voltage-dependent changes in the glutamate-dependent current, indicating that there are no branching connections from one of the uptake cycle states of the transporter (Fig. 3). Slow fluorescence changes are thus due to conformational changes that occur in certain states of EAAT3 but do not interfere with the uptake cycle. At present, we can only speculate about the molecular basis and functional consequences of this finding. A possible explanation of these slow processes might be large collective motions as recently reported by Jiang *et al.* (43). An alternative assumption is that these very slow fluorescence changes correspond to a slow gating process within the EAAT anion channel. This gating process has been initially described

in EAAT4 where slow changes in the anion to cation selectivity occur upon membrane depolarization. We also observed similar processes for EAAT3,[3] and the time and voltage dependences of these gating processes resemble the observed slow changes of the fluorescence signals (17).

Due to the slow changes of fluorescence amplitudes, it was impossible to obtain and interpret steady-state fluorescence values. We therefore determined fluorescence values at the end of a 200-ms pulse. After this time period, all processes within the uptake cycle will have reached steady-state conditions. Moreover, the additional slow processes that occur outside the uptake cycle and thus should not contribute to the measured fluorescence values will not have caused major alterations of the fluorescence levels.

We recently performed a detailed analysis of the effects of D117A on EAAT4 anion currents (19). Noise analysis demonstrated reduced unitary current amplitudes of D117A EAAT4 anion channels, and reversal potential measurements under bionic conditions indicated altered anion selectivity. These functional alterations supported direct modification of the EAAT4 anion conduction pathway by D117A. We reasoned that Asp-117 is in close proximity to the anion conduction pathway and that D117A alters anion channel open probabilities by directly modifying opening and closing transitions. We optimized rate constants in the kinetic scheme that is closely similar to the one shown in Fig. 6 against experimentally determined absolute open probabilities for WT and D117A EAAT4 at different voltages. This procedure revealed that the effect of D117A on EAAT4 gating can be well reproduced by exclusive modification of anion channel open probabilities.

We now studied the effects of the homologous mutation on EAAT3 using voltage clamp fluorometry. The use of EAAT3 permits direct measurements of glutamate uptake currents, and this parameter turned out to be crucial for our interpretation of the effects of D83A. Cysteine-substituted EAAT3 fluorescence, glutamate transport, and anion currents can be well represented by a kinetic scheme that is based on a model developed in a recent voltage clamp fluorometry study (23). We optimized this scheme by inserting anion channel states branching from certain states of the glutamate transport cycle. For WT EAAT3, rate constants within the uptake cycle were not modified. The glutamate transport cycle consists of many different steps, and some of them are outside the temporal resolution of our system. Moreover, the kinetic scheme encompasses too many rate constants to be accurately determined in separation. The resulting scheme is in good agreement with all our experimental data on WT. However, there is one published feature of EAAT3 for which the kinetic model fails to account. It is not able to correctly predict the high transport rates of EAAT3 for reverse transport at high external K^+ (44). Because our experiments were performed in the absence of external K^+, we accepted this limitation of the kinetic scheme.

The effects of D83A on fluorescence and anion current could be explained by modifying anion channel gating. However, these alterations predicted a reduction of the glutamate uptake rates to very low values and are thus in disagreement with experimental data (Fig. 4). Only by modification of translocation rates in the uptake cycle were we able to accurately describe all existing data, glutamate transport, anion currents, and fluorescence data. Our data thus indicate that D83A modifies translocation rates. These changes in translocation are supported by available crystal structures that place the homologous residue of Asp-83/Asp-117 to the TM2-TM3 loop between the trimerization and transport domains. By altering the hinge function of this region (19, 34, 45), D83A/D117A might affect the isomerization between inward and outward facing conformations.

The different outcome of the two studies on EAAT3 and EAAT4 is most likely not due to isoform-specific differences in anion channel function but rather caused by the separate experimental approaches. Anion channel properties are very well conserved between EAAT3 and EAAT4 with closely similar unitary conductance, selectivity, and open probabilities (33). EAAT4 differs from EAAT3 in very low glutamate transport rates (27). Changes in translocation processes might have less influence on anion channel gating in EAAT4 than in EAAT3. D83A is thus expected to exert effects on EAAT3 anion channels similar to those of D117A on EAAT4 anion channels. We conclude that D83A/D117A modifies substrate translocation and anion channel opening as well as anion conduction by EAAT3/EAAT4.

At present, the molecular basis of anion conduction in EAAT glutamate transporters is insufficiently understood. So far, only one point mutation, D117A, has been shown to modify unitary anion conduction rates in the outward (35) as well as in the inward facing conformation (34). Ser-74, the Glt_{Ph} residue homologous to Asp-83/Asp-117, projects into surrounding lipids rather than into possible conduction pathways. Moreover, D117A reduces unitary current amplitudes of EAAT4 anion channels by removing a negative charge. These two findings argue against a direct effect of D83A/D117A on anion conduction. A possible scenario that accounts for the effects of D83A on substrate translocation in EAAT3 and of D117A on anion conduction in EAAT4 is that anion channel formation is closely related to translocation. One might speculate that the anion pore opens upon moving the translocation domain between outward to inward facing conformations. Indeed, a recently reported high resolution structure of an intermediate conformation of Glt_{Ph} revealed an aqueous conduction pathway that might permit permeation of anions (32). By altering the translocation trajectory, D83A/D117A could not only affect substrate translocation and anion channel opening/closing but also the anion conduction pathway itself.

Acknowledgments—We thank Dr. M. Hediger for providing the expression construct for hEAAT3. We appreciate helpful discussions with Drs. Alexi Alekov, David Ewers, Peter Kovermann, Gabriel Stölting, and Nicole Schneider.

[3] D. Torres-Salazar, unpublished observation.

REFERENCES

1. Zerangue, N., and Kavanaugh, M. P. (1996) Flux coupling in a neuronal glutamate transporter. *Nature* **383,** 634–637
2. Levy, L. M., Warr, O., and Attwell, D. (1998) Stoichiometry of the glial

glutamate transporter GLT-1 expressed inducibly in a Chinese hamster ovary cell line selected for low endogenous Na^+-dependent glutamate uptake. *J. Neurosci.* **18,** 9620–9628
3. Danbolt, N. C. (2001) Glutamate uptake. *Prog. Neurobiol.* **65,** 1–105
4. Kanner, B. I. (2006) Structure and function of sodium-coupled GABA and glutamate transporters. *J. Membr. Biol.* **213,** 89–100
5. Grewer, C., Gameiro, A., Zhang, Z., Tao, Z., Braams, S., and Rauen, T. (2008) Glutamate forward and reverse transport: from molecular mechanism to transporter-mediated release after ischemia. *IUBMB Life* **60,** 609–619
6. Tanaka, K., Watase, K., Manabe, T., Yamada, K., Watanabe, M., Takahashi, K., Iwama, H., Nishikawa, T., Ichihara, N., Kikuchi, T., Okuyama, S., Kawashima, N., Hori, S., Takimoto, M., and Wada, K. (1997) Epilepsy and exacerbation of brain injury in mice lacking the glutamate transporter GLT-1. *Science* **276,** 1699–1702
7. Watase, K., Hashimoto, K., Kano, M., Yamada, K., Watanabe, M., Inoue, Y., Okuyama, S., Sakagawa, T., Ogawa, S., Kawashima, N., Hori, S., Takimoto, M., Wada, K., and Tanaka, K. (1998) Motor discoordination and increased susceptibility to cerebellar injury in GLAST mutant mice. *Eur. J. Neurosci.* **10,** 976–988
8. Peghini, P., Janzen, J., and Stoffel, W. (1997) Glutamate transporter EAAC-1-deficient mice develop dicarboxylic aminoaciduria and behavioral abnormalities but no neurodegeneration. *EMBO J.* **16,** 3822–3832
9. Aoyama, K., Suh, S. W., Hamby, A. M., Liu, J., Chan, W. Y., Chen, Y., and Swanson, R. A. (2006) Neuronal glutathione deficiency and age-dependent neurodegeneration in the EAAC1 deficient mouse. *Nat. Neurosci.* **9,** 119–126
10. Huang, Y. H., Dykes-Hoberg, M., Tanaka, K., Rothstein, J. D., and Bergles, D. E. (2004) Climbing fiber activation of EAAT4 transporters and kainate receptors in cerebellar Purkinje cells. *J. Neurosci.* **24,** 103–111
11. Bailey, C. G., Ryan, R. M., Thoeng, A. D., Ng, C., King, K., Vanslambrouck, J. M., Auray-Blais, C., Vandenberg, R. J., Bröer, S., and Rasko, J. E. (2011) Loss-of-function mutations in the glutamate transporter SLC1A1 cause human dicarboxylic aminoaciduria. *J. Clin. Investig.* **121,** 446–453
12. Fairman, W. A., Vandenberg, R. J., Arriza, J. L., Kavanaugh, M. P., and Amara, S. G. (1995) An excitatory amino-acid transporter with properties of a ligand-gated chloride channel. *Nature* **375,** 599–603
13. Wadiche, J. I., Amara, S. G., and Kavanaugh, M. P. (1995) Ion fluxes associated with excitatory amino acid transport. *Neuron* **15,** 721–728
14. Grewer, C., Watzke, N., Wiessner, M., and Rauen, T. (2000) Glutamate translocation of the neuronal glutamate transporter EAAC1 occurs within milliseconds. *Proc. Natl. Acad. Sci. U.S.A.* **97,** 9706–9711
15. Melzer, N., Biela, A., and Fahlke, Ch. (2003) Glutamate modifies ion conduction and voltage-dependent gating of excitatory amino acid transporter-associated anion channels. *J. Biol. Chem.* **278,** 50112–50119
16. Fairman, W. A., and Amara, S. G. (1999) Functional diversity of excitatory amino acid transporters: ion channel and transport modes. *Am. J. Physiol. Renal Physiol.* **277,** F481–F486
17. Melzer, N., Torres-Salazar, D., and Fahlke, Ch. (2005) A dynamic switch between inhibitory and excitatory currents in a neuronal glutamate transporter. *Proc. Natl. Acad. Sci. U.S.A.* **102,** 19214–19218
18. Vandenberg, R. J., Huang, S., and Ryan, R. M. (2008) Slips, leaks and channels in glutamate transporters. *Channels* **2,** 51–58
19. Kovermann, P., Machtens, J. P., Ewers, D., and Fahlke, Ch. (2010) A conserved aspartate determines pore properties of anion channels associated with excitatory amino acid transporter 4 (EAAT4). *J. Biol. Chem.* **285,** 23676–23686
20. Ryan, R. M., Mitrovic, A. D., and Vandenberg, R. J. (2004) The chloride permeation pathway of a glutamate transporter and its proximity to the glutamate translocation pathway. *J. Biol. Chem.* **279,** 20742–20751
21. Mannuzzu, L. M., Moronne, M. M., and Isacoff, E. Y. (1996) Direct physical measure of conformational rearrangement underlying potassium channel gating. *Science* **271,** 213–216
22. Cha, A., and Bezanilla, F. (1997) Characterizing voltage-dependent conformational changes in the Shaker K^+ channel with fluorescence. *Neuron* **19,** 1127–1140
23. Larsson, H. P., Tzingounis, A. V., Koch, H. P., and Kavanaugh, M. P. (2004) Fluorometric measurements of conformational changes in glutamate transporters. *Proc. Natl. Acad. Sci. U.S.A.* **101,** 3951–3956
24. Koch, H. P., and Larsson, H. P. (2005) Small-scale molecular motions accomplish glutamate uptake in human glutamate transporters. *J. Neurosci.* **25,** 1730–1736
25. Koch, H. P., Hubbard, J. M., and Larsson, H. P. (2007) Voltage-independent sodium-binding events reported by the 4B-4C loop in the human glutamate transporter excitatory amino acid transporter 3. *J. Biol. Chem.* **282,** 24547–24553
26. Larsson, H. P., Wang, X., Lev, B., Baconguis, I., Caplan, D. A., Vyleta, N. P., Koch, H. P., Diez-Sampedro, A., and Noskov, S. Y. (2010) Evidence for a third sodium-binding site in glutamate transporters suggests an ion/substrate coupling model. *Proc. Natl. Acad. Sci. U.S.A.* **107,** 13912–13917
27. Mim, C., Balani, P., Rauen, T., and Grewer, C. (2005) The glutamate transporter subtypes EAAT4 and EAATs 1–3 transport glutamate with dramatically different kinetics and voltage dependence but share a common uptake mechanism. *J. Gen. Physiol* **126,** 571–589
28. Lorenz, C., Pusch, M., and Jentsch, T. J. (1996) Heteromultimeric CLC chloride channels with novel properties. *Proc. Natl. Acad. Sci. U.S.A.* **93,** 13362–13366
29. Trotti, D., Rolfs, A., Danbolt, N. C., Brown, R. H., Jr., and Hediger, M. A. (1999) SOD1 mutants linked to amyotrophic lateral sclerosis selectively inactivate a glial glutamate transporter. *Nat. Neurosci.* **2,** 427–433
30. Torres-Salazar, D., and Fahlke, Ch. (2006) Intersubunit interactions in EAAT4 glutamate transporters. *J. Neurosci.* **26,** 7513–7522
31. Bergles, D. E., Tzingounis, A. V., and Jahr, C. E. (2002) Comparison of coupled and uncoupled currents during glutamate uptake by GLT-1 transporters. *J. Neurosci.* **22,** 10153–10162
32. Verdon, G., and Boudker, O. (2012) Crystal structure of an asymmetric trimer of a bacterial glutamate transporter homolog. *Nat. Struct. Mol. Biol.* **19,** 355–357
33. Torres-Salazar, D., and Fahlke, Ch. (2007) Neuronal glutamate transporters vary in substrate transport rate but not in unitary anion channel conductance. *J. Biol. Chem.* **282,** 34719–34726
34. Reyes, N., Ginter, C., and Boudker, O. (2009) Transport mechanism of a bacterial homologue of glutamate transporters. *Nature* **462,** 880–885
35. Boudker, O., Ryan, R. M., Yernool, D., Shimamoto, K., and Gouaux, E. (2007) Coupling substrate and ion binding to extracellular gate of a sodium-dependent aspartate transporter. *Nature* **445,** 387–393
36. Shimamoto, K., Lebrun, B., Yasuda-Kamatani, Y., Sakaitani, M., Shigeri, Y., Yumoto, N., and Nakajima, T. (1998) DL-*threo*-β-Benzyloxyaspartate, a potent blocker of excitatory amino acid transporters. *Mol. Pharmacol.* **53,** 195–201
37. Kanner, B. I., and Bendahan, A. (1982) Binding order of substrates to the sodium and potassium ion coupled L-glutamic acid transporter from rat brain. *Biochemistry* **21,** 6327–6330
38. Machtens, J. P., Fahlke, Ch., and Kovermann, P. (2011) Noise analysis to study unitary properties of transporter-associated ion channels. *Channels* **5,** 468–474
39. Leinenweber, A., Machtens, J. P., Begemann, B., and Fahlke, Ch. (2011) Regulation of glial glutamate transporters by C-terminal domains. *J. Biol. Chem.* **286,** 1927–1937
40. Wadiche, J. I., and Kavanaugh, M. P. (1998) Macroscopic and microscopic properties of a cloned glutamate transporter/chloride channel. *J. Neurosci.* **18,** 7650–7661
41. Gandhi, C. S., and Olcese, R. (2008) The voltage-clamp fluorometry technique. *Methods Mol. Biol.* **491,** 213–231
42. Machtens, J. P., Kovermann, P., and Fahlke, Ch. (2011) Substrate-dependent gating of anion channels associated with excitatory amino acid transporter 4. *J. Biol. Chem.* **286,** 23780–23788
43. Jiang, J., Shrivastava, I. H., Watts, S. D., Bahar, I., and Amara, S. G. (2011) Large collective motions regulate the functional properties of glutamate transporter trimers. *Proc. Natl. Acad. Sci. U.S.A.* **108,** 15141–15146
44. Zhang, Z., Tao, Z., Gameiro, A., Barcelona, S., Braams, S., Rauen, T., and Grewer, C. (2007) Transport direction determines the kinetics of substrate transport by the glutamate transporter EAAC1. *Proc. Natl. Acad. Sci. U.S.A.* **104,** 18025–18030
45. Yernool, D., Boudker, O., Jin, Y., and Gouaux, E. (2004) Structure of a glutamate transporter homologue from *Pyrococcus horikoshii*. *Nature* **431,** 811–818